bacteria

MDPI

Article

New Insights on the Glyphosate-Degrading Enzymes C-P Lyase and Glyphosate Oxidoreductase Based on Bioinformatics

Marina Giannakara and Vassiliki Lila Koumandou *

Genetics Laboratory, Department of Biotechnology, Agricultural University of Athens, Iera Odos 75, 11855 Athens, Greece; marinagiann14@outlook.com

* Correspondence: koumandou@aua.gr; Tel.: +30-210-529-4645

Abstract: Bioremediation, the degradation of environmental pollutants by living organisms, has immense potential to lead to a greener planet. Bioinformatics analysis can contribute to the identification of novel microorganisms, which biodegrade contaminants, or of participating proteins and enzymes, and the elucidation of the complex metabolic pathways involved. In this study, we focus on C-P lyase and glyphosate oxidoreductase (Gox), two enzymes which degrade glyphosate, a widely used pesticide. Amino acid sequences of the two enzymes were collected from a broad range of microorganisms using the KEGG database and BLAST. Based on this, we identified additional lineages, with putative glyphosate-degrading activity, for which no glyphosate-degrading species have been reported yet. The conserved residues in each enzyme were identified via multiple alignments and mapped onto the 3D structures of the enzymes, using PyMOL, leading to novel insights into their function. As the experimental structure of Gox is still unknown, we created structural models based on three different programs and compared the results. This approach can be used to yield insights into the characteristics of potential glyphosate-degrading enzymes. Given the limited information available, such a step is important to gain further knowledge about them, which can contribute to their application in bioremediation in the future.

Keywords: glyphosate; C-P lyase; glyphosate oxidoreductase; biodegradation; bioinformatics; phylogenetics

Citation: Giannakara, M.; Koumandou, V.L. New Insights on the Glyphosate-Degrading Enzymes C-P Lyase and Glyphosate Oxidoreductase Based on Bioinformatics. *Bacteria* **2024**, *3*, 314–329. https://doi.org/10.3390/bacteria3040021

Academic Editors: Debasis Mitra, Marika Pellegrini, Leonard Koolman and Bart C. Weimer

Received: 23 July 2024
Revised: 13 September 2024
Accepted: 29 September 2024
Published: 2 October 2024

1. Introduction

Glyphosate, *N*-(phosphonomethyl)glycine, is an active ingredient in many widely used, broad-spectrum herbicides (e.g., Roundup^{TM}). It is a synthetic amino acid analogue of glycine incorporating a phosphonic acid [1]. It inhibits enolpyruvylshikimate-3-phosphate synthase (EPSP synthase), resulting in the inhibition of the shikimate pathway, which is essential for the biosynthesis of aromatic amino acids in plants [2].

Glyphosate has been characterized as a safe compound by the European Food Safety Authority (EFSA) for human health, animals, and the environment, as "no critical areas of concern" were confirmed. Additionally, the European Chemicals Agency (ECHA) does not classify glyphosate as carcinogenic or possibly carcinogenic [3]. On the other hand, it is considered as "probably carcinogenic" to humans (Group 2A) according to the International Agency for Research on Cancer (IARC) [1] and it is labeled as "toxic to aquatic life with long lasting effects" as per the Hazard Statements of the Globally Harmonized System of Classification and Labelling of Chemicals (GHS) [1]. Glyphosate was an approved pesticide until December 2023 in the E.U. [3], where its use was recently extended for 10 more years [4].

Nevertheless, there is increasing concern about the accumulation of pesticide residues and their metabolites in soils and food crops. In soil sampled from agricultural sites throughout the E.U. and other cooperating countries, glyphosate and its metabolite alpha-amino-3-hydroxy-5-methyl-4-isoxazolepropionic acid (AMPA) were among the most frequently detected substances and also among those with the highest concentrations [5].

A case study in central Germany yielded similar results, as glyphosate and AMPA were detected at the highest concentrations in surface water and topsoil samples [6]. Concerns have also been raised about the persistence of glyphosate and its metabolite AMPA in soil, especially in fields where glyphosate-based herbicides have been extensively used [3,7], its potential to bioaccumulate in terrestrial organisms [8], and its impact on crop health [3], while it has also led to glyphosate-resistant weeds [9]. Both compounds are transported off site with rainfall, contaminating surface water, hedgerows, and adjacent non-treated fields [7,8].

In particular, glyphosate can affect the microbial population, and hence, have an impact on plant-beneficial microbes [10] and cause metabolic changes in plants, even at low doses [11]. Glyphosate and its salt form, isopropylamine (IPA), also act as chelating agents by binding to metal cations necessary for plant nutrition [12]. Additionally, studies have shown potential negative effects on insects; i.e., rendering insects more prone to infections, inhibiting the production of melanin, disturbing their gut microbiome [13–16], and leading to a low responsiveness to sucrose [17] and impaired aversive learning [18]. Aquatic organisms are also affected: in zebrafish and other commercial fish, such as Nile tilapia, glyphosate has been linked to developmental problems [19], cardiovascular toxicity [20], oxidative stress and anxiety [21], and kidney disfunction [22]. Glyphosate impacts aquatic ecosystems via changes in the abundance and composition of freshwater picoplanktonic populations [23] and certain species of marine phytoplankton [24]. Glyphosate can have a negative impact on mammals by altering gene expression and affecting DNA methylation in human cells [25–27]. The glyphosate-based herbicide Roundup^{TM}, glyphosate, and AMPA can indirectly cause DNA damage by inducing reactive oxygen species (ROS) production in human peripheral blood mononuclear cells [28]. In addition, exposure of human lymphocytes to glyphosate in higher concentrations (200 µmol/L) than those normally found in the environment (20–40 µmol/L) demonstrated genotoxic effects [29]. It has also been associated with increased urinary glyphosate and AMPA levels in humans [30], which, in turn, have been associated with longer telomere length in leukocytes [31]. Low chronic maternal exposure to glyphosate has also been associated with reduced immune response in mice [32].

The degradation of glyphosate can be either biotic, by microorganisms in both aerobic and anaerobic conditions, or abiotic, by Mn-containing minerals [33], and depends on many factors, e.g., whether it is found in water or soil, soil properties, weather conditions, and cultivated plants in the area. Regarding its degradation rate, half-life estimates range from 5 to 180 days [34].

There is limited current knowledge about the pathways involved in phosphonate degradation, including glyphosate, their regulation, and the relevant enzymes [35]. Three enzymes have been reported to degrade glyphosate: C-P lyase, which cleaves the bond after phosphorus; and glyphosate oxidoreductase (Gox) and glycine oxidase (GO), which both cleave the C-N bond. The last two enzymes produce the same products but their function is based on a different mechanism (Figure 1).

C-P lyase is a protein complex that consists of two copies each of four proteins (PhnG, PhnH, PhnI, PhnJ) and one ATP-binding subunit, PhnK. The degradation of glyphosate by C-P lyase, which takes place under inorganic phosphate (Pi) deficiency [35], results in the production of sarcosine and phosphate. The C-P lyase complex is part of the C-P lyase pathway, which converts phosphonate into PRPP (5-phosphoribosyl-a-1-diphosphate) using ATP [35]. According to the literature, it is widely present across bacteria, and shows broad substrate specificity, as it cleaves the C-P bond of organophosphonates [36]. At first, the tertiary structure of the complex was determined without PhnK (PDB accession number: 4XB6) [37]. A few years later, PhnK was also included in the complex via single-particle cryogenic electron microscopy, which provided valuable insights into the interactions of PhnK with the core complex and the conformational changes before and after utilizing ATP (PDB accession number: 7Z19, with ATP: 7Z18), and also, with PhnL in various conformations (PhnK/PhnL dual ABC dimer, PDB accession numbers: 7Z15, 7Z16) [38].

PhnJ is the active site of the enzyme (Figure S1). It contains an Fe_4S_4 complex and a Zn molecule, which is stabilized by three conserved Cys residues (Cys241, Cys244, and Cys266), found within the conserved motif CX2CX21C. Two more residues are important for the reaction mechanism of the complex: Gly32 and Cys272 [39]. Due to the presence of the fourth conserved Cys residue, it can be included as part of the aforementioned motif, namely, as CX2CX21CX5C [39]. Cys272 is responsible for the generation of a thiyl radical, which cleaves the C-P bond of 5-phosphoribosyl-1-phosphonate. Notably, PhnJ does not contain the signature radical SAM enzyme motif (CX3CX2C), which stabilizes the Fe_4S_4 complex [39]. A second potential active site is located between PhnJ and PhnI, which includes the residues His328 and His333 (PhnI) and His108 (PhnJ). Four further domains (Figure S1) have been described [37]:

- CMD: C-terminal mini domain (PhnJ);
- CID: Central insertion domain (PhnJ), which could participate in the binding of PhnK to PhnJ;
- BBD: Beta barrel domain (PhnI);
- NTD: N-terminal domain (PhnI).

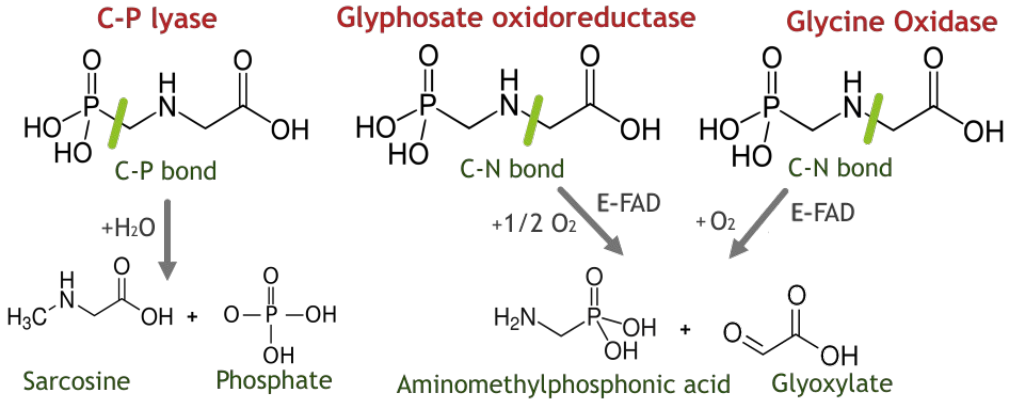

Figure 1. The enzymes degrading glyphosate, their reaction mechanisms, and the resulting products. Glyphosate image from https://en.m.wikipedia.org/wiki/File:Glyphosate.svg (accessed on 28 November 2021).

It has been proposed that not all C-P lyases are specific to glyphosate, and that C-P lyase of *Eschericha coli* is an example of an (amino)alkylphosphate-specific enzyme without glyphosate-degrading activity [35,40]. For this reason, there is the hypothesis that two different types of independently induced C-P lyases exist [35]. However, later research on *Ochrobactrum anthropi* and *Achromobacter* sp. [41] could not provide evidence for the hypothesis of two distinct C-P lyases (Sviridov A, personal communication).

The glyphosate oxidoreductase (Gox) gene was first characterized from *Achromobacter* sp. LBAA, a bacterial strain isolated in a glyphosate waste treatment facility, as part of a Monsanto patent [42], in order to construct glyphosate-resistant plants. Gox is a monomeric FAD-dependent enzyme, cleaving the C-N bond of glyphosate and yielding glyoxylate and the metabolite AMPA. It is speculated that the reduction of FAD takes place in the active site of the enzyme by glyphosate [42]. There is no known experimental structure of Gox, although a computed structural model is available [43].

Glycine oxidase (GO) is the third enzyme known to degrade glyphosate. Several GO structures are available in the PDB (e.g., 3IF9, 1NG4 and 1RYI from *Bacillus subtilis*). It is a homotetrameric enzyme and its substrates include glycine, neutral D-amino acids, and sarcosine. Similar to Gox, it is an FAD-dependent enzyme and it cleaves the C-N bond, yielding the same degradation products: AMPA and glyoxylate. However, Gox and GO show low sequence identity [2] and, based on oxygen utilization, appear to have a different reaction mechanism: oxygen reduction in Gox does not result in the production

of hydrogen peroxide, which is the case for GO [2,42]. Several studies have focused on engineering GO in order to enhance its glyphosate-degrading activity [2,44–47].

Given the negative consequences of glyphosate, in this study we look at the characteristics of the proteins of the glyphosate-degrading enzymes at a sequence level as a way to understand and optimize their function, by utilizing bioinformatics tools. As GO has been extensively studied and improved through mutagenesis, we focus on C-P lyase and Gox. Further insights into the enzymatic degradation of glyphosate by bacteria can contribute to the eventual application of bioremediation techniques for a faster removal of glyphosate from affected areas.

2. Materials and Methods

Information on the bacterial species reported to degrade glyphosate and the pathways or enzymes involved in this activity was collected from relevant references in PubMed [48] and ScienceDirect [49] (Table 1). These databases, along with PDB [50], were also used to find the already-available information on enzymes responsible for glyphosate degradation, namely, Gox, C-P lyase, and GO.

For C-P lyase, the amino acid sequences for each subunit of the complex were collected using the KEGG Orthology (KO) database [51] and the following entries: PhnJ: K06163, PhnI: K06164, PhnH: K06165, PhnG: K06166, and PhnK: K05781. The available sequences were parsed in such a way that a wide variety of representatives from across the bacterial kingdom were included; the selection was performed manually, using the taxonomy option of the KO entry and selecting at least one representative per family. The selected amino acid sequences are available in the Supplementary Dataset in folder "C-P lyase". The sequence selected from each taxonomical group was random and we also included the sequence of *E. coli*. MUSCLE [52] was used for the multiple alignments, and the highly conserved residues were marked onto the 3D structure using PyMOL (linux version 2.5.2) [53]. The absolutely conserved residues were selected based on Jalview [54] (scoring 11); residues in positions with a Jalview score of 10 were also selected, which reflects that, despite variation, physicochemical properties are conserved [54]. The ScanProsite tool (https://prosite.expasy.org/scanprosite/, accessed on 15 March 2022) was used to search for motifs in the PhnJ sequences of the C-P lyase complex.

As there is no KEGG Orthology (KO) group for Gox, BLASTp [55] searches for orthologs in other species were performed using as a query the Gox amino acid sequence of *Ochrobactrum* sp. G-1 (ACZ58378.1). Two different databases were used:

- The nr database (BLASTp_nr), which includes all non-redundant GenBank CDS translations and also entries from PDB, SwissProt, PIR, and PRF, excluding environmental samples from WGS projects.
- RefSeq (BLASTp_ref), which contains only curated entries, i.e., one representative or "Select" transcript for every protein-coding gene, based on specific criteria [55].

Two different BLASTp searches were performed, with default settings, for each database (Table S1), one without any filters (BLASTp_nr_NOGROUP, BLASTp_ref_NOGROUP) and one for each bacterial group (BLASTp_nr_GROUP, BLASTp_ref_GROUP), as defined by Jun et al. [56], aiming at better sampling of more bacterial representatives. The selection of the resulting sequences for BLASTp_nr_NOGROUP and BLASTp_ref_NOGROUP was based on the first 100 sequences with the lowest E-value for each protein query. For the BLASTp_nr_NOGROUP, the highest E-value was 3×10^{-128} and for the BLASTp_ref_NOGROUP 1×10^{-127} (available in Supplementary Dataset). For BLASTp_nr_GROUP and BLASTp_ref_GROUP, the results with the lowest E-value for each protein query from each bacterial group were selected. MUSCLE [52] was used for the multiple alignments.

The Gox 3D structure was computed using I-TASSER [57] and Phyre2 [58], which are based on homology modeling, as well as AlphaFold Colab, which performs ab initio prediction [59]. The default settings were used. A general comparison of the results was made by aligning the structures with PyMOL. The results were assessed using QMEANDisCo, which is part of SWISS-MODEL [60].

3. Results and Discussion

3.1. Distribution of Bacterial Species Previously Reported to Degrade Glyphosate

In the literature, 42 different bacterial species have been reported to degrade glyphosate (Table 1). The majority of the species belong to α-, β-, and γ-proteobacteria, a smaller number to bacilli and actinobacteria, and some to bacteroidetes (Figure 2). The enzymes or genes involved in glyphosate degradation have been identified only in some research papers. In most cases, the possible mechanism was inferred based on the products resulting after glyphosate consumption by the bacteria, specifically, based on the presence of sarcosine (indicating C-P lyase activity) or AMPA (indicating Gox activity). In addition to the three known glyphosate-degrading proteins, the presence of a class II EPSPS synthase-encoding gene (*aroA* gene) has also been reported, although the experimental structure of the protein is not yet known and no further experiments were carried out to test and validate the activity of *aroA* [61]. Consequently, the knowledge about the genes and the structure or mechanism of the enzymes involved in glyphosate degradation is still limited.

Table 1. Bacterial species reported to degrade glyphosate. Depending on the evidence of glyphosate degradation in each paper, "G" represents the discovery of the responsible gene, "P" the presence of the degradation product, and hyphen (-) a decrease in the amount of glyphosate.

Group	Genus, Species	Evidence	Products/Genes Detected	Reference
actinobacteria	*Arthrobacter* sp. GLP-1	P	Sarcosine	[62]
actinobacteria	*Streptomycete* sp. StC	P	Sarcosine	[63]
actinobacteria	*Streptomyces* sp. StA	P	Sarcosine	[63]
actinobacteria	*Rhodococcus soli* G41	G	*soxB* gene	[64]
actinomycetes	*Arthrobacter atrocyaneus* ATCC 13752	P	AMPA	[65]
bacilli	*Geobacillus caldoxylosilyticus* T20	P	AMPA	[66]
bacilli	*Bacillus cereus* CB4	P	AMPA, glyoxylate, sarcosine, formaldehyde	[67]
bacilli	*Lysinibacillus sphaericus*	P	Free phosphorus concentration, glycine	[68]
bacilli	*Bacillus aryabhattai* FACU	G	*goxB* gene	[69]
bacilli	*Bacillus. cereus* 6 P	-	Conversion of glyphosate to polyphosphate	[70]
bacteroidetes	*Flavobacterium* sp. GD1	P	AMPA	[33]
bacteroidetes	*Chryseobacterium* sp. Y16C	P	AMPA	[71]
αctinobacteria	*Arthrobacter atrocyaneus* ATCC 13752	P	AMPA	[65]
α-proteobacteria	*Agrobacterium radiobacter*	P	AMPA	[33]
α-proteobacteria	*Ochrobactrum anthropi* GPK 3	P	AMPA	[72]
α-proteobacteria	*Ochrobactrum* sp. GDOS	P	AMPA	[73]
α-proteobacteria	*Ochrobactrum* sp. G1	G	*gox* gene	[42]
α-proteobacteria	*Agrobacterium radiobacter* SW9	P	AMPA	[74]
α-proteobacteria	*Rhizobiaceae meliloti* 1021	G	Homology to part of the *phn* gene cluster of *E. coli*	[75]
α-proteobacteria	*Ochrobactrum* sp. GDOS	P	AMPA	[73]
α-proteobacteria	*Agrobacterium tumefaciens* CHLDO	G	*phn* gene cluster	[76]
α-proteobacteria	*Ochrobactrum haematophilum* SR	-	-	
α-proteobacteria	*Ochrobactrum intermedium* Sq20	G, P	Sarcosine, glycine, *aroA* gene (class II EPSPS)	[61]
β-proteobacteria	*Comamonas odontotermitis* P2	G	*gox* and *phnJ* genes	[77]
β-proteobacteria	*Achromobacter* sp. strain MPK 7A	P	Sarcosine	[72]
β-proteobacteria	*Achromobacter* sp. Kg 16	P	AcGP(*N*-acetylglyphosate), possibly AMPA	[72]
β-proteobacteria	*Achromobacter* Group V D (*Agrobacterium* sp. LW9)	P	AMPA	[74]

Table 1. *Cont.*

Group	Genus, Species	Evidence	Products/Genes Detected	Reference
β-proteobacteria	*Achromobacter* sp. MPS 12A	P	Methane, sarcosine, glycine	[41]
β-proteobacteria	*Alcaligenes* sp. GL	P	Sarcosine	[78]
β-proteobacteria	*Burkholderia vietnamiensis* strain AQ5-12	-	-	[79]
β-proteobacteria	*Achromobacter denitrificans* SOS5	-	-	[76]
β-proteobacteria	*Achromobacter insolitus* SOR2	-	-	[76]
β-proteobacteria	*Achromobacter xylosoxidans* SOS3	-	-	[76]
β-proteobacteria	*Achromobacter insolitus* str Kg 19 (VKM B-3295)	G	*phnJ* gene	[80]
γ-proteobacteria	*Pseudomonas* sp. LBr	P	AMPA, a very small amount of glycine 5%	[81]
γ-proteobacteria	*Providencia rettgeri* GDB 1	P	AMPA	[82]
γ-proteobacteria	*Pseudomonas* sp. 4ASW	P	Sarcosine	[83]
γ-proteobacteria	*Enterobacter cloacae* K7	P	Sarcosine, glycine	[84]
γ-proteobacteria	*Enterobacter* sp. Bisph2	-	-	[85]
γ-proteobacteria	*Pseudomonas pseudomallei* 22	G, P	Phosphotransferase genes *glpA* and *glpB*	[86]
γ-proteobacteria	*Pseudomonas* sp. GLC11	-	-	[87]
γ-proteobacteria	*Pseudomonas* sp. PG2982	P	Sarcosine	[88]
γ-proteobacteria	*Pseudomonas* sp. SG-1		Glyphosate concentration decreased	[89]
γ-proteobacteria	*Pseudomonas nitroreducens* TR3	-	-	[76]

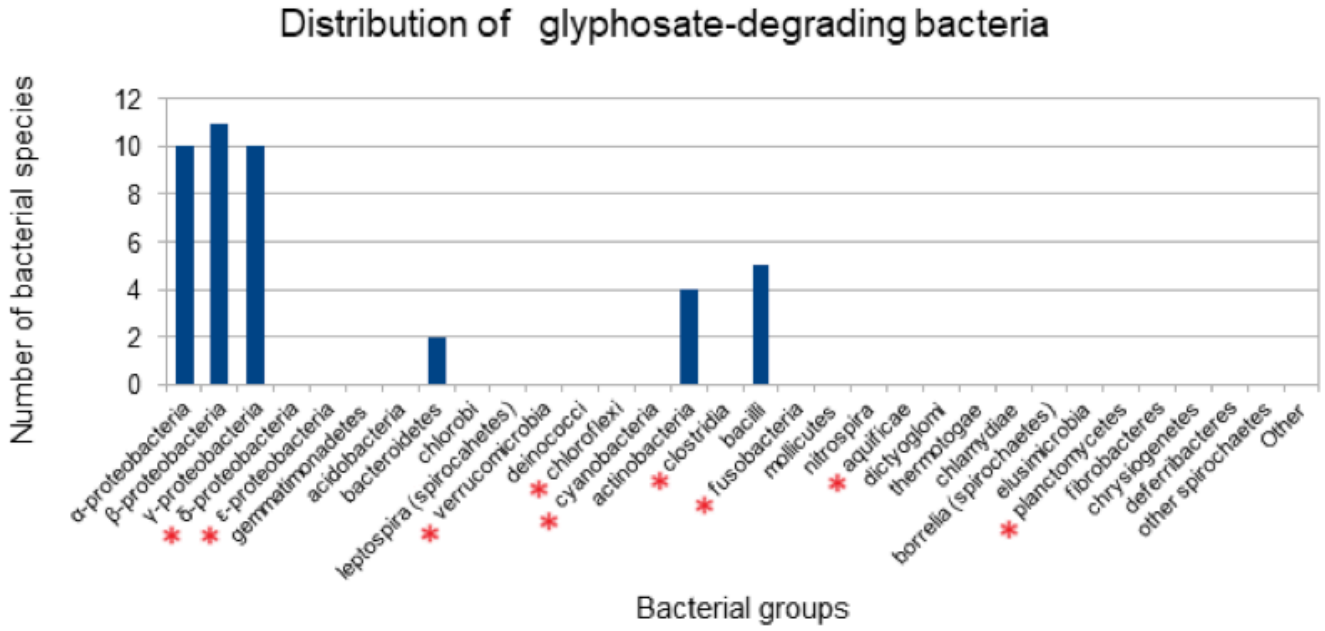

Figure 2. Distribution of the bacterial species reported to degrade glyphosate, based on the data available in Table 1 (blue bars). The red stars (*) indicate the additional lineages, for which no glyphosate-degrading species have been reported yet, and which, based on our KEGG and BLASTp searches, may have glyphosate-degrading activity. Further research is required to confirm this activity.

3.2. Protein Conservation across Prokaryotes

The entries in KEGG for the proteins of the C-P lyase complex belong to a wide range of bacterial phyla (Figure S2A,C). The bacterial species expected to express C-P lyase based on KEGG (Figure S2) belong to more bacterial groups than the bacterial species reported in the literature as degrading glyphosate (Table 1, Figure 2). This suggests that there are more bacterial species with the potential to degrade glyphosate that have not been studied

yet; it may also simply show conserved function against phosphonates, which may or may not include glyphosate. More specifically, the additional bacterial groups found after our KEGG search are actinobacteria, chloroflexi, clostridia, cyanobacteria, δ-proteobacteria, and ε-proteobacteria.

For Gox, as there were no relevant KEGG entries, we performed BLASTp and NCBI [90] keyword searches. We were able to find only 13 annotated Gox proteins. Those belong to α-proteobacteria, β-proteobacteria, and bacilli, but many of them are partial and the organism is not yet known (Table S2). The BLASTp search results included mostly FAD-dependent oxidoreductases, D-amino acid dehydrogenases, and glycine oxidases. Based on the percent identity of the BLASTp results, the sequences with the general term "FAD-dependent oxidases" showed higher sequence similarity to the annotated Gox sequences than the "D-amino acid dehydrogenases" and GOs; GOs demonstrated the lowest average percent identity (Figure S3).

The BLASTp searches for Gox without filtering per group showed fewer bacterial groups than those reported in the literature, namely, sequences only from α-, β-, and γ-proteobacteria (Figures S2B, S4 and S5). However, when we performed the searches per bacterial group, the diversity of the results increased significantly (Figure S2B,D). In addition to the aforementioned groups, we found entries belonging to verrucomicrobia, fusobacteria, aquificae, and planctomycetes. Figures S4 and S5 show distinctive changes in the phylogenetic distribution of the BLASTp results. Although there are no known motifs of Gox responsible for glyphosate degradation, these BLASTp results are worth investigating further for such a potential.

3.3. Conserved Residues in C-P Lyase

Multiple alignments of each of the proteins of the C-P lyase complex revealed a large number of conserved residues (Figure S6). The results were compared with the C-P lyase complex of *E. coli* (4X6B), which has been extensively studied previously. Although *E. coli* cannot degrade glyphosate, PhnI and PhnJ proteins show a high degree of conservation with glyphosate-degrading bacteria (*Sinorhizobium meliloti)* [75]. A detailed description of the discovered conserved residues, previous mentions in the bibliography, and the secondary structure of each region are found in Table 2. The position of the highly conserved residues on the tertiary structure of the enzyme is highlighted in Figure S7.

From our alignments, many previously unreported conserved residues were discovered, which could be significant for the function of the enzyme. Some of these residues are close to the active site of PhnJ, or are part of the domains CMD, CID (PhnJ), BBD, and NTD (PhnI). The function of certain conserved residues has been suggested previously and, by proximity, we can deduce the function of several of the newly identified conserved residues. For example, residues G208, R209, G47, G49, V125, T50, and G51 were previously found, using molecular docking, to interact with AMPA via hydrogen bonds [43]; we find conservation of these residues, which lends support to their important role, and we suggest that they also surround and may help stabilize the Fe_4S_4 cluster. Also, in addition to the Cys residues surrounding Zn, Gly245 is conserved right next to Cys244, suggesting that this may also contribute to stabilizing Zn. The loop containing the universally conserved Gly32 also contains two more conserved residues (Pro31, Gln34), which could participate in receiving the intermediate radical while catalyzing the substrate formed by SAM. The fact that the CMD domain only contains three conserved residues matches the hypothesis that it might detach from the core of PhnJ during interaction [37]. Conserved His residues in the interface of PhnJ and PhnI also coordinate a second Zn molecule. From our alignments, more residues were found to be conserved in this region in both the PhnJ and PnhI proteins, suggesting that they contribute to the overall structure around Zn. The large number of highly conserved residues supports the assumption that this could be a potential second active site of the C-P lyase complex [37]. PhnG is generally not highly conserved. However, there are a small number of conserved residues in the C-terminal part, which is reported to interact with PhnI [47]. Notably, there is a set of conserved residues, remote

from the rest of the C-P lyase core complex, which does not seem to interact with any substrate or other proteins of the complex.

Table 2. Conserved residues of the C-P lyase complex of *E. coli*, identified in alignments from this study, compared to those described in the literature, for the proteins PhnJ, PhnI, and PhnG. The blue highlighted residues are the unique ones found in this study, which are not mentioned in the literature. The green highlighted residues are those mentioned in the literature which were not highly conserved in our alignments (i.e., scores 10 or 11 based on Jalview, see methods). The asterisk (*) denotes that P36 is at the border of loop2 and a b-sheet that precedes the loop.

PhnJ			
Secondary Structure	**MUSCLE Alignment Residues Identified in Alignments from This Study**	**Conserved Residues as Given by Seweryn et al. [37]**	**Residues Predicted In Silico to Participate in Interaction with AMPA and GLP [43]. HB: H Bond HI: Hydrophobic Interaction**
Residues Surrounding the Fe_4S_4 Cluster			
loop 1	A207, G208, R209, E210	-	AMPA: G208 (HB), R209 (HB)
loop 2	P36 *, P40, P43 Near the cluster: G47, G49	-	AMPA: G47 (HB), G49 (HB)
loop 3	Q124, V125, P126	-	AMPA: V125 (HB)
helix 1	T50, G51, G52 More distant: Q54	-	AMPA: T50 (HB), G51 (HB)
Residues surrounding Zn			
loop 4	G245	C241, C244	Y250 (HI); more distant to Zn, S267 (HB)
β sheet loop		C266	
helix6		C272	
Residues surrounding universally conserved residue G32			
loop 5	P31, Q34	G32	
CID—Central insertion domain—contacts both of the central PhnI molecules			
loop 3	L131, E135		
helix 2	H145	129–169	
helix 3	Y150, L157		
CMD—C-terminal mini domain—stabilized by Zn ion and conserved C residues			
β hairpin	E253 (loop), G260 (β sheet)	236–281	
His108 coordinate Zn ion with 2 His from PhnI			
loop 6	R107, R109 More distant: P111, F112, L115	H108	GLP: H108 (HB), R109 (HI)
loop 7	P187	-	
helix 5	P189, D192	-	GLP: P189 (HI)
loop 8	D70, Q71, G72	-	GLP: Q71 (HB)
Two of the residues (PhnI His328 and His333) coordinate the zinc ion directly PhnJ His108, PhnI His328, and PhnI His333 are located in a cavity between PhnI and PhnJ			
β strand 1	K67, V68, I69, D70		
loop	Q71, G72		
β strand 2	I104, Q105, R107		
loop	R109	(H108)	
loop (Bhatt)	P174, F232		Y171 (HI)
PhnI			

Table 2. *Cont.*

Secondary structure	MUSCLE alignment Residues not reported by [37], identified in alignments from this study		Conserved residues [37]
Residues surrounding the Fe_4S_4 cluster			
loop 1 loop 2	A55	G278	-
NTD—N-terminal domain			
β strand 1	Y2, A4		1–88
helix 2	G7, G8, A11		
helix 3	E51		
loop 1	A55		
helix 4	A60, A63, Q66		
loop 4	G69		
helix 5	E73, A74, R82, T84		
β strand 2	K87		
His108 coordinate Zn ion with 1 His from PhnJ			
loop 5	P332		-
helix 6	Y334		H333
helix 7	F325, K330 Further away: D318, G324		H328
C-terminal			
helix 8	R189, R198, Y209, R213		188–318
loop 6	G214, G216, H219		
β strand 3	G223, E224, R226, G228		
β strand 4	G246, E252		
β strand 5	G272, G274		
loop 7	G278		
helix 9	E281, K283, M287		
helix 10	F312, H316		
helix 11	D318		
PhnG			
Secondary structure	**MUSCLE alignment Residues not reported by [37], identified in alignments from this study**		**Conserved residues [37]**
β-hairpin and C-terminal helix form a molecular clamp that connects to a groove in PhnI			
β strand 1	G63	-	-
β strand 2	G80	-	-
helix	A96, D99, A100	-	-
loop	V139, F141	-	-

Most residues which are reported to be conserved in the literature and play a significant role in the function of the enzyme were also conserved in our alignments. However, five residues of PhnJ that are expected to interact with glyphosate and AMPA in silico [43], and

three of the residues participating in the conserved Cys motif of PhnJ, are not absolutely conserved in our alignment. This discrepancy may be because we used more sequences in the alignments compared to Seweryn et al. [37]. Cys244 and Cys266 are present in 96% of the sequences, but they are replaced by amino acids with the same properties (Ser or Thr and Ile or Thr, respectively). The most important change is noticed for Cys272, which plays a significant role in the function of the enzyme as it is the last Cys residue of the conserved motif CX2CX21CX5C [37]. According to our results, position 310 of the multiple alignment, which corresponds to Cys272 of *E. coli*, was not absolutely conserved in all sequences and it was replaced by either Met or Leu. The sequences that did not correspond to Cys in this position were:

- cyb—*Synechococcus* sp. JA-2-3B'a(2-13) (bacteroidota)—Met269;
- muh—*Mucilaginibacter celer* HYN0043 (bacteroidota)—Leu276;
- shv—*Salinicoccus halodurans* H3B36 (bacilli)—Met269;
- crn—*Carnobacterium* sp. 17-4 (bacilli)—Met27.

This raised the question of whether the motif is present in another part of the sequences, and whether the rest of the sequences actually have the conserved motif. Although Cys was conserved in this position for the rest of the entries, in some cases the number of residues between the conserved Cys was different than that determined for the CX2CX21CX5C motif. For this reason, we searched for the motif CX2CX21CX5C in all of our sequences: it was found in only 77 out of 93 PhnJ sequences in total. The 16 sequences in which the motif was not present are shown in Table S3. However, as the typical motif for SAM enzymes is CX3CX2C, and variations of this motif (CX4CX2C, CX5CX2C, CX3CX3C, CX14CX2C) can also be observed [91], we also searched for these motifs in our sequences. The CX3CX2C SAM typical motif was not found in any of the sequences, and none of the sequences without the CX2CX21CX5C motif contain any alternative motif. Only two sequences contained the alternative motif CX5CX2C and, interestingly, both have the motif of PhnJ too: hbe—*Halomonas beimenensis* NTU-111 (γ-proteobacteria), and stea—*Sporolactobacillus terrae* DRG1 (bacilli).

3.4. Structure of Gox

There is no available experimental structure for Gox in PDB. The only attempt at a structural approach used Phyre2, based on the amino acid sequence of *Ochrobactrum* sp. G1 (ACZ58378.1) [43]. We created structural models based on AlphaFold Colab and I-TASSER, which present similarities with Phyre2 (Figure 3). According to the evaluation based on QMEANDisCo (Figure S8), the best model is produced by AlphaFold, a conclusion that is supported by the recent assessment of structure prediction models (CASP14), referring to the performance of AlphaFold [92]. Phyre2 and AlphaFold show significant differences in specific regions of the predicted structure, which end up around the surface of the structure (Figures 3 and S9). Based on the docking results of Bhatt et al. [43], glyphosate is expected to bind to the center of the protein. There are slight differences between the three models; for example, R358 is part of a loop in I-TASSER but on a beta sheet in AlphaFold and Phyre2, and M388 is in a helix in Phyre2, but part of a loop in I-TASSER and AlphaFold. As glyphosate is a small molecule and these accumulative small changes may alter the shape of the binding site, this can have an impact on the functionality of the proposed binding site on each calculated structure. It is also not known yet if Gox acts as a monomer or dimer/polymer; in the latter case, the peripheral structure may also play a role in subunit interactions.

The residues hypothesized by Bhatt et al. [43] to interact with glyphosate were not consistently conserved in our multiple alignments (Table 3). None of the residues were conserved for all datasets, and only N47 and R358 were highly conserved for the results of both BLASTp_nr_NOGROUP and BLASTp_ref_NOGROUP. Residues like V16, A43, and M388 were conserved in less than 50% of the sequences in all 4 alignments. Therefore, further structural and docking studies are needed in order to obtain a more precise model of the Gox active site.

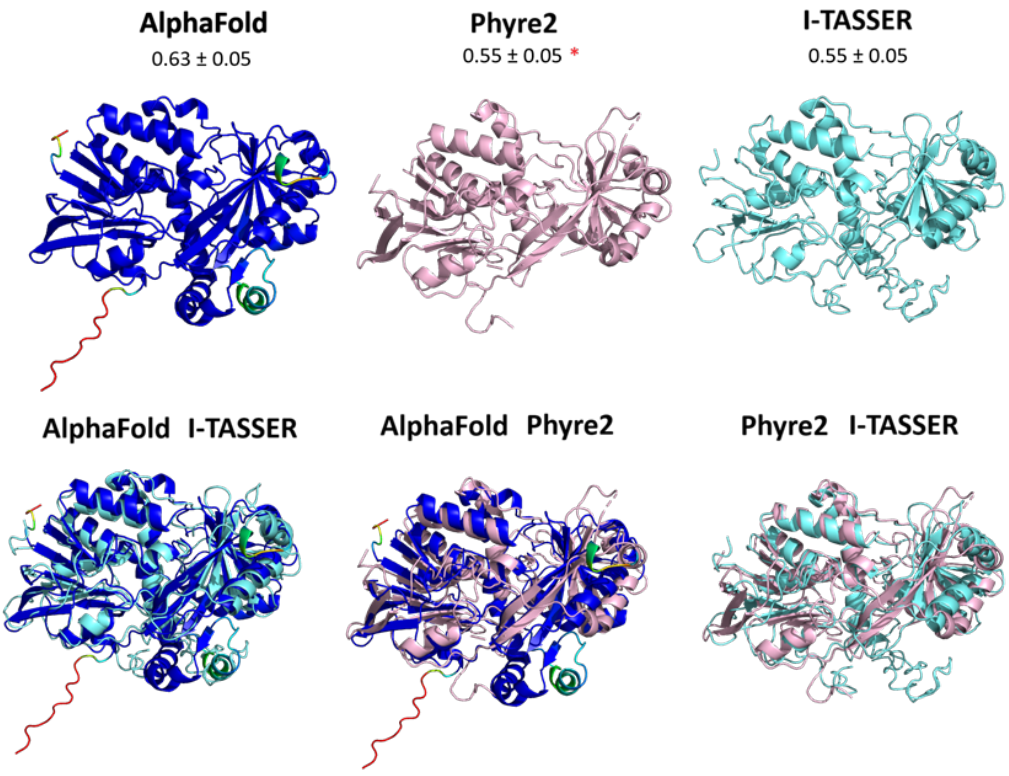

Figure 3. The computed 3D structures of Gox from *Ochrobactrum* sp. G-1 (NCBI Accession number ACZ58378.1) using AlphaFold, Phyre2, and I-TASSER. Top panel: individual models with the ranking for each program (local quality estimate, QMEANDisCo global ranking). * Although the performance of I-TASSER and Phyre2 seems to be the same, it is important to note that part of the structure is missing in Phyre2, which has a significantly low score in AlphaFold and I-TASSER (Figure S8). Bottom panel: Structures aligned using PyMOL.

Table 3. Conservation of residues hypothesized by Bhatt et al. [43] to interact with glyphosate in our multiple alignments. Green crosses show the residues of the computed binding site that are highly conserved in each of our own multiple alignments (corresponding to a Jalview score of 10 or 11).

Bhatt et al., 2021	BLASTp_nr_ NOGROUP	BLASTp_ref_ NOGROUP	BLASTp_nr_ GROUP	BLASTp_ref_ GROUP
G14		+		+
I15				
V16				
A43		+		
S44				
N47	+	+		
R358	+	+		
G384				
G387	+			+
M388				

4. Conclusions

In this study, based on BLAST and KEGG searches, additional lineages were identified, which are worth investigation for glyphosate-degrading activity, as no glyphosate-degrading species have been reported from these lineages yet. Furthermore, additional conserved residues have been identified for each protein of the C-P lyase complex. Further studies would be useful to determine their role in the structure and function of the complex. Interestingly, Cys272 of PhnJ from *E. coli*, an important residue for the function of the active site of C-P lyase, is overall conserved but not present in all PhnJ sequences, raising the question of whether those PhnJ sequences have an alternative mechanism or if they have a

different activity. Given the limited information on glyphosate degradation through the C-P lyase pathway [35], further studies of the C-P lyase pathway and the participating genes are needed, e.g., regarding the efficiency of the enzyme and the dependence of the *phn* gene expression on Pi deficiency.

Oxidoreductases are a large group of versatile enzymes [93] with conserved domains of low sequence similarity. There is a big research gap in the amino acid sequences of proteins known to degrade glyphosate, as most studies of glyphosate-degrading activity are based on detecting the degradation products with no further analysis at sequence level or identification of the responsible protein (Table 1). Bioinformatics analysis of already available biological data can contribute to the knowledge about Gox proteins. There are only a few annotated Gox proteins and we lack information about their reaction mechanism, the participating residues, and even the biological function in the bacteria which express them. The BLAST results show that Gox sequences are more similar to "FAD-dependent oxidases". An experimentally determined Gox structure is not yet available and the binding site of glyphosate to the protein is not known yet. Here, we compare models based on three programs. The majority of the residues previously proposed to interact with glyphosate are not highly conserved in our alignments. Therefore, it would be interesting to create a more detailed structure in silico, which can be used for docking, in order to study the interacting residues and to search for enzymes with similar active sites. This could lead to the discovery of enzymes with higher efficiency, being better candidates to be applied in situ for the remediation of contaminated sites.

Supplementary Materials: The following supporting information can be downloaded at: https://www.mdpi.com/article/10.3390/bacteria3040021/s1, Figure S1: Tertiary structure of the C-P lyase core complex; Figure S2: Distribution of C-P lyase and Gox across the major bacterial lineages; Figure S3: Average percent identity values between the resulting amino acid sequences from our BLASTp searches and the annotated Gox proteins; Figure S4: Phylogenetic distribution of the BLASTp results against the nr database using the Gox ACZ58378.1 as a query sequence; Figure S5: Phylogenetic distribution of the BLASTp results against the Refseq database using the Gox ACZ58378.1 as a query sequence; Figure S6: Conserved residues in C-P lyase deduced from the MUSCLE alignments in this study, shown per protein subunit; Figure S7: Conserved residues in C-P lyase marked on the 3D structure of the enzyme; Figure S8: Scoring of the computed Gox structures; Figure S9: Phyre2 and AlphaFold show significant differences in specific regions of the predicted structure; Table S1: Methodology of the choice of the amino acid sequences for Gox homologs; Table S2: The annotated Gox protein types in NCBI. Table S3. KEGG entries of the PhnJ sequences which lack the motifs CX2CX21C and CX2CX21CX5C.

Author Contributions: Conceptualization, M.G. and V.L.K.; methodology, M.G. and V.L.K.; investigation, M.G.; data curation, M.G.; writing—original draft preparation, M.G.; writing—review and editing, V.L.K.; visualization, M.G.; supervision, V.L.K. All authors have read and agreed to the published version of the manuscript.

Funding: This research received no external funding.

Institutional Review Board Statement: Not applicable.

Informed Consent Statement: Not applicable.

Data Availability Statement: Publicly available datasets were analyzed in this study. Details of sequences studied, alignments, and models available in the Supplementary Dataset.

Conflicts of Interest: The authors declare no conflicts of interest.

References

1. PubChem PubChem Compound Summary for CID 3496, Glyphosate. Available online: https://pubchem.ncbi.nlm.nih.gov/compound/3496 (accessed on 10 June 2022).
2. Pedotti, M.; Rosini, E.; Molla, G.; Moschetti, T.; Savino, C.; Vallone, B.; Pollegioni, L. Glyphosate Resistance by Engineering the Flavoenzyme Glycine Oxidase. *J. Biol. Chem.* **2009**, *284*, 36415–36423. [CrossRef] [PubMed]

3. Kanissery, R.; Gairhe, B.; Kadyampakeni, D.; Batuman, O.; Alferez, F. Glyphosate: Its Environmental Persistence and Impact on Crop Health and Nutrition. *Plants* **2019**, *8*, 499. [CrossRef] [PubMed]
4. EFSA EFSA Explains the Scientific Assessment of Glyphosate. Available online: https://www.efsa.europa.eu/en/factsheets/efsa-explains-scientific-assessment-glyphosate (accessed on 15 February 2024).
5. Silva, V.; Mol, H.G.J.; Zomer, P.; Tienstra, M.; Ritsema, C.J.; Geissen, V. Pesticide Residues in European Agricultural Soils—A Hidden Reality Unfolded. *Sci. Total Environ.* **2019**, *653*, 1532–1545. [CrossRef]
6. Tauchnitz, N.; Kurzius, F.; Rupp, H.; Schmidt, G.; Hauser, B.; Schrödter, M.; Meissner, R. Assessment of Pesticide Inputs into Surface Waters by Agricultural and Urban Sources—A Case Study in the Querne/Weida Catchment, Central Germany. *Environ. Pollut.* **2020**, *267*, 115186. [CrossRef]
7. Bento, C.P.M.; van der Hoeven, S.; Yang, X.; Riksen, M.M.J.P.M.; Mol, H.G.J.; Ritsema, C.J.; Geissen, V. Dynamics of Glyphosate and AMPA in the Soil Surface Layer of Glyphosate-Resistant Crop Cultivations in the Loess Pampas of Argentina. *Environ. Pollut.* **2019**, *244*, 323–331. [CrossRef]
8. Pelosi, C.; Bertrand, C.; Bretagnolle, V.; Coeurdassier, M.; Delhomme, O.; Deschamps, M.; Gaba, S.; Millet, M.; Nélieu, S.; Fritsch, C. Glyphosate, AMPA and Glufosinate in Soils and Earthworms in a French Arable Landscape. *Chemosphere* **2022**, *301*, 134672. [CrossRef]
9. Baek, Y.; Bobadilla, L.K.; Giacomini, D.A.; Montgomery, J.S.; Murphy, B.P.; Tranel, P.J. Evolution of Glyphosate-Resistant Weeds. *Rev. Environ. Contam. Toxicol.* **2021**, *255*, 93–128. [CrossRef]
10. Fuchs, B.; Saikkonen, K.; Damerau, A.; Yang, B.; Helander, M. Herbicide Residues in Soil Decrease Microbe-Mediated Plant Protection. *Plant Biol.* **2023**, *25*, 571–578. [CrossRef] [PubMed]
11. Kováčik, J.; Novotný, V.; Bujdoš, M.; Dresler, S.; Hladký, J.; Babula, P. Glyphosate Does Not Show Higher Phytotoxicity than Cadmium: Cross Talk and Metabolic Changes in Common Herb. *J. Hazard. Mater.* **2020**, *383*, 121250. [CrossRef]
12. Mertens, M.; Höss, S.; Neumann, G.; Afzal, J.; Reichenbecher, W. Glyphosate, a Chelating Agent—Relevant for Ecological Risk Assessment? *Environ. Sci. Pollut. Res.* **2018**, *25*, 5298–5317. [CrossRef]
13. Smith, D.F.Q.; Camacho, E.; Thakur, R.; Barron, A.J.; Dong, Y.; Dimopoulos, G.; Broderick, N.A.; Casadevall, A. Glyphosate Inhibits Melanization and Increases Susceptibility to Infection in Insects. *PLoS Biol.* **2021**, *19*, e3001182. [CrossRef] [PubMed]
14. Motta, E.V.S.; Raymann, K.; Moran, N.A. Glyphosate Perturbs the Gut Microbiota of Honey Bees. *Proc. Natl. Acad. Sci. USA* **2018**, *115*, 10305–10310. [CrossRef] [PubMed]
15. Motta, E.V.S.; Mak, M.; De Jong, T.K.; Powell, J.E.; O'Donnell, A.; Suhr, K.J.; Riddington, I.M.; Moran, N.A. Oral or Topical Exposure to Glyphosate in Herbicide Formulation Impacts the Gut Microbiota and Survival Rates of Honey Bees. *Appl. Environ. Microbiol.* **2020**, *86*, e01150-20. [CrossRef] [PubMed]
16. Blot, N.; Veillat, L.; Rouzé, R.; Delatte, H. Glyphosate, but Not Its Metabolite AMPA, Alters the Honeybee Gut Microbiota. *PLoS ONE* **2019**, *14*, e0215466. [CrossRef] [PubMed]
17. Thompson, L.J.; Stout, J.C.; Stanley, D.A. Contrasting Effects of Fungicide and Herbicide Active Ingredients and Their Formulations on Bumblebee Learning and Behaviour. *J. Exp. Biol.* **2023**, *226*, jeb245180. [CrossRef]
18. Nouvian, M.; Foster, J.J.; Weidenmüller, A. Glyphosate Impairs Aversive Learning in Bumblebees. *Sci. Total Environ.* **2023**, *898*, 165527. [CrossRef]
19. Liu, Z.; Shangguan, Y.; Zhu, P.; Sultan, Y.; Feng, Y.; Li, X.; Ma, J. Developmental Toxicity of Glyphosate on Embryo-Larval Zebrafish (Danio Rerio). *Ecotoxicol. Environ. Saf.* **2022**, *236*, 113493. [CrossRef]
20. Lu, J.; Wang, W.; Zhang, C.; Xu, W.; Chen, W.; Tao, L.; Li, Z.; Cheng, J.; Zhang, Y. Characterization of Glyphosate-Induced Cardiovascular Toxicity and Apoptosis in Zebrafish. *Sci. Total Environ.* **2022**, *851*, 158308. [CrossRef]
21. Faria, M.; Bedrossiantz, J.; Ramírez, J.R.R.; Mayol, M.; García, G.H.; Bellot, M.; Prats, E.; Garcia-Reyero, N.; Gómez-Canela, C.; Gómez-Oliván, L.M.; et al. Glyphosate Targets Fish Monoaminergic Systems Leading to Oxidative Stress and Anxiety. *Environ. Int.* **2021**, *146*, 106253. [CrossRef]
22. Abdelmagid, A.D.; Said, A.M.; Abd El-Gawad, E.A.; Shalaby, S.A.; Dawood, M.A.O. Glyphosate-Induced Liver and Kidney Dysfunction, Oxidative Stress, Immunosuppression in Nile Tilapia, but Ginger Showed a Protection Role. *Vet. Res. Commun.* **2023**, *47*, 445–455. [CrossRef]
23. Sabio y García, C.A.; Schiaffino, M.R.; Lozano, V.L.; Vera, M.S.; Ferraro, M.; Izaguirre, I.; Pizarro, H. New Findings on the Effect of Glyphosate on Autotrophic and Heterotrophic Picoplankton Structure: A Microcosm Approach. *Aquat. Toxicol.* **2020**, *222*, 105463. [CrossRef] [PubMed]
24. Wang, C.; Lin, X.; Li, L.; Lin, S. Differential Growth Responses of Marine Phytoplankton to Herbicide Glyphosate. *PLoS ONE* **2016**, *11*, e0151633. [CrossRef]
25. Duforestel, M.; Nadaradjane, A.; Bougras-Cartron, G.; Briand, J.; Olivier, C.; Frenel, J.S.; Vallette, F.M.; Lelièvre, S.A.; Cartron, P.F. Glyphosate Primes Mammary Cells for Tumorigenesis by Reprogramming the Epigenome in a TET3-Dependent Manner. *Front. Genet.* **2019**, *10*, 885. [CrossRef]
26. Woźniak, E.; Reszka, E.; Jabłońska, E.; Balcerczyk, A.; Broncel, M.; Bukowska, B. Glyphosate Affects Methylation in the Promoter Regions of Selected Tumor Suppressors as Well as Expression of Major Cell Cycle and Apoptosis Drivers in PBMCs (in Vitro Study). *Toxicol. Vitr.* **2020**, *63*, 104736. [CrossRef] [PubMed]

27. Woźniak, E.; Reszka, E.; Jabłońska, E.; Michałowicz, J.; Huras, B.; Bukowska, B. Glyphosate and Ampa Induce Alterations in Expression of Genes Involved in Chromatin Architecture in Human Peripheral Blood Mononuclear Cells (In Vitro). *Int. J. Mol. Sci.* **2021**, *22*, 2966. [CrossRef] [PubMed]
28. Woźniak, E.; Sicińska, P.; Michałowicz, J.; Woźniak, K.; Reszka, E.; Huras, B.; Zakrzewski, J.; Bukowska, B. The Mechanism of DNA Damage Induced by Roundup 360 PLUS, Glyphosate and AMPA in Human Peripheral Blood Mononuclear Cells—Genotoxic Risk Assessement. *Food Chem. Toxicol.* **2018**, *120*, 510–522. [CrossRef]
29. Tarboush, N.A.; Almomani, D.H.; Khabour, O.F.; Azzam, M.I. Genotoxicity of Glyphosate on Cultured Human Lymphocytes. *Int. J. Toxicol.* **2022**, *41*, 126–131. [CrossRef]
30. Lucia, R.M.; Huang, W.L.; Pathak, K.V.; McGilvrey, M.; David-Dirgo, V.; Alvarez, A.; Goodman, D.; Masunaka, I.; Odegaard, A.O.; Ziogas, A.; et al. Association of Glyphosate Exposure with Blood DNA Methylation in a Cross-Sectional Study of Postmenopausal Women. *Environ. Health Perspect.* **2022**, *130*, 047001. [CrossRef]
31. Cosemans, C.; Van Larebeke, N.; Janssen, B.G.; Martens, D.S.; Baeyens, W.; Bruckers, L.; Den Hond, E.; Coertjens, D.; Nelen, V.; Schoeters, G.; et al. Glyphosate and AMPA Exposure in Relation to Markers of Biological Aging in an Adult Population-Based Study. *Int. J. Hyg. Environ. Health* **2022**, *240*, 113895. [CrossRef]
32. Buchenauer, L.; Junge, K.M.; Haange, S.B.; Simon, J.C.; von Bergen, M.; Hoh, A.L.; Aust, G.; Zenclussen, A.C.; Stangl, G.I.; Polte, T. Glyphosate Differentially Affects the Allergic Immune Response across Generations in Mice. *Sci. Total Environ.* **2022**, *850*, 157973. [CrossRef]
33. la Cecilia, D.; Maggi, F. Analysis of Glyphosate Degradation in a Soil Microcosm. *Environ. Pollut.* **2018**, *233*, 201–207. [CrossRef] [PubMed]
34. Mercurio, P.; Flores, F.; Mueller, J.F.; Carter, S.; Negri, A.P. Glyphosate Persistence in Seawater. *Mar. Pollut. Bull.* **2014**, *85*, 385–390. [CrossRef] [PubMed]
35. Sviridov, A.V.; Shushkova, T.V.; Ermakova, I.T.; Ivanova, E.V.; Epiktetov, D.O.; Leontievsky, A.A. Microbial Degradation of Glyphosate Herbicides (Review). *Appl. Biochem. Microbiol.* **2015**, *51*, 188–195. [CrossRef]
36. Hove-jensen, B.; Zechel, D.L. Utilization of Glyphosate as Phosphate Source: Biochemistry and Genetics of Bacterial Carbon-Phosphorus Lyase. *Biotechnol. Mol. Biol. Rev.* **2014**, *78*, 176–197. [CrossRef]
37. Seweryn, P.; Van, L.B.; Kjeldgaard, M.; Russo, C.J.; Passmore, L.A.; Hove-Jensen, B.; Jochimsen, B.; Brodersen, D.E. Structural Insights into the Bacterial Carbon-Phosphorus Lyase Machinery. *Nature* **2015**, *525*, 68–72. [CrossRef]
38. Amstrup, S.K.; Ong, S.C.; Sofos, N.; Karlsen, J.L.; Skjerning, R.B.; Boesen, T.; Enghild, J.J.; Hove-Jensen, B.; Brodersen, D.E. Structural Remodelling of the Carbon–Phosphorus Lyase Machinery by a Dual ABC ATPase. *Nat. Commun.* **2023**, *14*, 1001. [CrossRef]
39. Kamat, S.S.; Raushel, F.M. PhnJ—A Novel Radical SAM Enzyme from the C–P Lyase Complex. *Perspect Sci.* **2015**, *4*, 32–37. [CrossRef]
40. Kononova, S.V.; Trutko, S.M.; Laurinavichus, K.S. Detection of C-P-Lyase Activity in a Cell-Free Extract of *Escherichia Coli*. *Appl. Biochem. Microbiol.* **2007**, *43*, 394–398. [CrossRef]
41. Sviridov, A.V.; Shushkova, T.V.; Zelenkova, N.F.; Vinokurova, N.G.; Morgunov, I.G.; Ermakova, I.T.; Leontievsky, A.A. Distribution of Glyphosate and Methylphosphonate Catabolism Systems in Soil Bacteria *Ochrobactrum anthropi* and *Achromobacter* Sp. *Appl. Microbiol. Biotechnol.* **2012**, *93*, 787–796. [CrossRef]
42. Barry, G.F.; Kishore, G.M. Glyphosate Tolerant Plants. US Patent 5463175, 31 October 1995.
43. Bhatt, P.; Joshi, T.; Bhatt, K.; Zhang, W.; Huang, Y.; Chen, S. Binding Interaction of Glyphosate with Glyphosate Oxidoreductase and C–P Lyase: Molecular Docking and Molecular Dynamics Simulation Studies. *J. Hazard. Mater.* **2021**, *409*, 124927. [CrossRef]
44. Yao, P.; Lin, Y.; Wu, G.; Lu, Y.; Zhan, T.; Kumar, A.; Zhang, L.; Liu, Z. Improvement of Glycine Oxidase by DNA Shuffling, and Site-Saturation Mutagenesis of F247 Residue. *Int. J. Biol. Macromol.* **2015**, *79*, 965–970. [CrossRef] [PubMed]
45. Zhan, T.; Zhang, K.; Chen, Y.; Lin, Y.; Wu, G.; Zhang, L.; Yao, P.; Shao, Z.; Liu, Z. Improving Glyphosate Oxidation Activity of Glycine Oxidase from *Bacillus cereus* by Directed Evolution. *PLoS ONE* **2013**, *8*, e79175. [CrossRef] [PubMed]
46. Zhang, K.; Guo, Y.; Yao, P.; Lin, Y.; Kumar, A.; Liu, Z.; Wu, G.; Zhang, L. Characterization and Directed Evolution of BliGO, a Novel Glycine Oxidase from *Bacillus licheniformis*. *Enzym. Microb. Technol.* **2016**, *85*, 12–18. [CrossRef] [PubMed]
47. Qin, Y.; Wu, G.; Guo, Y.; Ke, D.; Yin, J.; Wang, D.; Fan, X.; Liu, Z.; Ruan, L.; Hu, Y. Engineered Glyphosate Oxidase Coupled to Spore-Based Chemiluminescence System for Glyphosate Detection. *Anal. Chim. Acta* **2020**, *1133*, 39–47. [CrossRef] [PubMed]
48. National Library of Medicine; National Institutes of Health; U.S. Department of Health and Human Services PubMed. Available online: https://pubmed.ncbi.nlm.nih.gov/ (accessed on 12 December 2021).
49. Elsevier, B.V. ScienceDirect. Available online: https://www.sciencedirect.com/ (accessed on 10 June 2022).
50. Berman, H.M.; Westbrook, J.; Feng, Z.; Gilliland, G.; Bhat, T.N.; Weissig, H.; Shindyalov, I.N.; Bourne, P.E. The Protein Data Bank. *Nucleic Acids Res.* **2000**, *28*, 235–242. [CrossRef]
51. Kanehisa Laboratories KEGG: Kyoto Encyclopedia of Genes and Genomes. Available online: https://www.kegg.jp/kegg/ (accessed on 15 June 2021).
52. Edgar, R.C. MUSCLE: Multiple Sequence Alignment with High Accuracy and High Throughput. *Nucleic Acids Res.* **2004**, *32*, 1792–1797. [CrossRef]
53. *The PyMOL Molecular Graphics System*, Version 2.5.2; Schrödinger, LLC.: New York, NY, USA, 2021. Available online: https://pymol.org/support.html (accessed on 11 November 2023).

54. Waterhouse, A.M.; Procter, J.B.; Martin, D.M.A.; Clamp, M.; Barton, G.J. Jalview Version 2-A Multiple Sequence Alignment Editor and Analysis Workbench. *Bioinformatics* **2009**, *25*, 1189–1191. [CrossRef]
55. Madden Thomas The BLAST Sequence Analysis Tool In The NCBI Handbook [Internet]. Available online: https://www.ncbi.nlm.nih.gov/books/NBK153387/ (accessed on 20 February 2024).
56. Jun, S.R.; Sims, G.E.; Wu, G.A.; Kim, S.H. Whole-Proteome Phylogeny of Prokaryotes by Feature Frequency Profiles: An Alignment-Free Method with Optimal Feature Resolution. *Proc. Natl. Acad. Sci. USA* **2010**, *107*, 133–138. [CrossRef]
57. Roy, A.; Kucukural, A.; Zhang, Y. I-TASSER: A Unified Platform for Automated Protein Structure and Function Prediction. *Nat. Protoc.* **2010**, *5*, 725–738. [CrossRef]
58. Kelley, L.A.; Mezulis, S.; Yates, C.M.; Wass, M.N.; Sternberg, M.J.E. The Phyre2 Web Portal for Protein Modeling, Prediction and Analysis. *Nat. Protoc.* **2015**, *10*, 845–858. [CrossRef]
59. Mirdita, M.; Schütze, K.; Moriwaki, Y.; Heo, L.; Ovchinnikov, S.; Steinegger, M. ColabFold: Making Protein Folding Accessible to All. *Nat. Methods* **2022**, *19*, 679–682. [CrossRef] [PubMed]
60. Studer, G.; Rempfer, C.; Waterhouse, A.M.; Gumienny, G.; Haas, J.; Schwede, T. QMEANDisCo—Distance Constraints Applied on Model Quality Estimation. *Bioinformatics* **2020**, *36*, 1765–1771. [CrossRef]
61. Firdous, S.; Iqbal, S.; Anwar, S.; Jabeen, H. Identification and Analysis of 5-Enolpyruvylshikimate-3-Phosphate Synthase (EPSPS) Gene from Glyphosate-Resistant Ochrobactrum Intermedium Sq20. *Pest. Manag. Sci.* **2018**, *74*, 1184–1196. [CrossRef] [PubMed]
62. Kertesz, M.; Elgorriaga, A.; Amrhein, N. Evidence for Two Distinct Phosphonate-Degrading Enzymes (C-P Lyases) in *Arthrobacter* Sp. GLP-1. *Biodegradation* **1991**, *2*, 53–59. [CrossRef]
63. Obojska, A.; Lejczak, B.; Kubrak, M. Degradation of Phosphonates by Streptomycete Isolates. *Appl. Microbiol. Biotechnol.* **1999**, *51*, 872–876. [CrossRef] [PubMed]
64. Nguyen, T.N.; Vo, V.T.; Nguyen, T.H.P.; Kiefer, R. Isolation and Optimization of a Glyphosate-Degrading *Rhodococcus soli* G41 for Bioremediation. *Arch. Microbiol.* **2022**, *204*, 252. [CrossRef] [PubMed]
65. Pipke, R.; Amrheint, N. Degradation of the Phosphonate Herbicide Glyphosate by *Arthrobacter atrocyaneus* ATCC 13752. *Appl. Environ. Microbiol.* **1988**, *54*, 1293–1296. [CrossRef]
66. Obojska, A.; Ternan, N.G.; Lejczak, B.; Kafarski, P.; McMullan, G. Organophosphonate Utilization by the Thermophile *Geobacillus caldoxylosilyticus* T20. *Appl. Environ. Microbiol.* **2002**, *68*, 2081–2084. [CrossRef]
67. Fan, J.; Yang, G.; Zhao, H.; Shi, G.; Geng, Y.; Hou, T.; Tao, K. Isolation, Identification and Characterization of a Glyphosate-Degrading Bacterium, *Bacillus cereus* CB4, from Soil. *J. Gen. Appl. Microbiol.* **2012**, *58*, 263–271. [CrossRef]
68. González-Valenzuela, L.E.; Dussán, J. Molecular Assessment of Glyphosate-Degradation Pathway via Sarcosine Intermediate in *Lysinibacillus sphaericus*. *Environ. Sci. Pollut. Res.* **2018**, *25*, 22790–22796. [CrossRef]
69. Elarabi, N.I.; Abdelhadi, A.A.; Ahmed, R.H.; Saleh, I.; Arif, I.A.; Osman, G.; Ahmed, D.S. *Bacillus aryabhattai* FACU: A Promising Bacterial Strain Capable of Manipulate the Glyphosate Herbicide Residues. *Saudi J. Biol. Sci.* **2020**, *27*, 2207–2214. [CrossRef] [PubMed]
70. Acosta-Cortés, A.G.; Martinez-Ledezma, C.; López-Chuken, U.J.; Kaushik, G.; Nimesh, S.; Villarreal-Chiu, J.F. Polyphosphate Recovery by a Native *Bacillus cereus* Strain as a Direct Effect of Glyphosate Uptake. *ISME J.* **2019**, *13*, 1497–1505. [CrossRef] [PubMed]
71. Zhang, W.; Li, J.; Zhang, Y.; Wu, X.; Zhou, Z.; Huang, Y.; Zhao, Y.; Mishra, S.; Bhatt, P.; Chen, S. Characterization of a Novel Glyphosate-Degrading Bacterial Species, *Chryseobacterium* Sp. Y16C, and Evaluation of Its Effects on Microbial Communities in Glyphosate-Contaminated Soil. *J. Hazard. Mater.* **2022**, *432*, 128689. [CrossRef] [PubMed]
72. Ermakova, I.T.; Shushkova, T.V.; Sviridov, A.V.; Zelenkova, N.F.; Vinokurova, N.G.; Baskunov, B.P.; Leontievsky, A.A. Organophosphonates Utilization by Soil Strains of *Ochrobactrum anthropi* and *Achromobacter* Sp. *Arch. Microbiol.* **2017**, *199*, 665–675. [CrossRef]
73. Hadi, F.; Mousavi, A.; Noghabi, K.A.; Tabar, H.G.; Salmanian, A.H. New Bacterial Strain of the Genus *Ochrobactrum* with Glyphosate-Degrading Activity. *J. Environ. Sci. Health B* **2013**, *48*, 208–213. [CrossRef]
74. Mcauliffe, K.S.; Hallas, L.E.; Kulpa, C.F. Glyphosate Degradation by *Agrobacterium radiobacter* Isolated from Activated Sludge. *J. Ind. Microbiol.* **1990**, *6*, 219–221. [CrossRef]
75. Parker, G.F.; Higgins, T.P.; Hawkes, T.; Robson, R.L. *Rhizobium* (*Sinorhizobium*) *meliloti phn* Genes: Characterization and Identification of Their Protein Products. *J. Bacteriol.* **1999**, *181*, 389–395. [CrossRef]
76. Masotti, F.; Garavaglia, B.S.; Piazza, A.; Burdisso, P.; Altabe, S.; Gottig, N.; Ottado, J. Bacterial Isolates from Argentine Pampas and Their Ability to Degrade Glyphosate. *Sci. Total Environ.* **2021**, *774*, 145761. [CrossRef]
77. Firdous, S.; Iqbal, S.; Anwar, S. Optimization and Modeling of Glyphosate Biodegradation by a Novel *Comamonas odontotermitis* P2 through Response Surface Methodology. *Pedosphere Int. J.* **2020**, *30*, 618–627. [CrossRef]
78. Lerbs, W.; Stock, M.; Parthier, B. Physiological Aspects of Glyphosate Degradation in *Alcaligenes Spec*. Strain GL. *Arch. Microbiol.* **1990**, *153*, 146–150. [CrossRef]
79. Manogaran, M.; Shukor, M.Y.; Yasid, N.A.; Khalil, K.A.; Ahmad, S.A. Optimisation of Culture Composition for Glyphosate Degradation by *Burkholderia vietnamiensis* Strain AQ5-12. *3Biotech* **2018**, *8*, 108. [CrossRef] [PubMed]
80. Tarlachkov, S.V.; Epiktetov, D.O.; Sviridov, A.V.; Shushkova, T.V.; Ermakova, I.T.; Leontievsky, A.A. Draft Genome Sequence of Glyphosate-Degrading *Achromobacter insolitus* Strain Kg 19 (VKM B-3295), Isolated from Agricultural Soil. *Microbiol. Resour. Announc.* **2020**, *9*. [CrossRef] [PubMed]

81. Jacob, G.S.; Garbow, J.R.; Hallas, L.E.; Kimack, N.M.; Kishore, G.M.; Schaefer, J. Metabolism of glyphosate in *Pseudomonas* sp. strain LBr. *Appl. Environ. Microbiol.* **1988**, *54*, 2953–2958. [CrossRef]
82. Xu, B.; Sun, Q.J.; Lan, J.C.W.; Chen, W.M.; Hsueh, C.C.; Chen, B.Y. Exploring the Glyphosate-Degrading Characteristics of a Newly Isolated, Highly Adapted Indigenous Bacterial Strain, *Providencia rettgeri* GDB 1. *J. Biosci. Bioeng.* **2019**, *128*, 80–87. [CrossRef]
83. Dick, R.E.; Quinn, J.P. Control of glyphosate uptake and metabolism in *Pseudomonas* sp. 4ASW. *FEMS Microbiol. Lett.* **1995**, *134*, 177–182. [CrossRef]
84. Kryuchkova, Y.V.; Burygin, G.L.; Gogoleva, N.E.; Gogolev, Y.V.; Chernyshova, M.P.; Makarov, O.E.; Fedorov, E.E.; Turkovskaya, O.V. Isolation and Characterization of a Glyphosate-Degrading Rhizosphere Strain, *Enterobacter cloacae* K7. *Microbiol. Res.* **2014**, *169*, 99–105. [CrossRef]
85. Benslama, O.; Boulahrouf, A. High-Quality Draft Genome Sequence of *Enterobacter* Sp. Bisph2, a Glyphosate-Degrading Bacterium Isolated from a Sandy Soil of Biskra, Algeria. *Genom. Data* **2016**, *8*, 61–66. [CrossRef]
86. Peñaloza-Vazquez, A.; Mena, G.L.; Herrera-Estrella, L.; Bailey, A.M. Cloning and sequencing of the genes. involved in glyphosate utilization by *Pseudomonas pseudomallei*. *Appl. Environ. Microbiol.* **1995**, *61*, 538–543. [CrossRef]
87. Selvapandiyan, A.; Bhatnagar, R.K. Isolation of a Glyphosate-Metabolising *Pseudomonas*: Detection, Partial Purification and Localisation of Carbon-Phosphorus Lyase. *Appl. Microbiol. Biotechnol.* **1994**, *40*, 876–882. [CrossRef]
88. Kishore, G.M.; Jacob, G.S. Degradation of Glyphosate by *Pseudomonas* Sp. PG2982 via a Sarcosine Intermediate. *J. Biol. Chem.* **1987**, *262*, 12164–12168. [CrossRef]
89. Talbot, H.W.; Johnson, L.M.; Munnecke, D.M. Glyphosate Utilization by *Pseudomonas* Sp. and *Alcaligenes* Sp. Isolated from Environmental Sources. *Curr. Microbiol.* **1984**, *10*, 255–259. [CrossRef]
90. Bethesda (MD): National Library of Medicine (US)-National Center for Biotechnology Information National Center for Biotechnology Information (NCBI). Available online: https://www.ncbi.nlm.nih.gov/ (accessed on 14 November 2023).
91. Nicolet, Y. Structure–Function Relationships of Radical SAM Enzymes. *Nat. Catal.* **2020**, *3*, 337–350. [CrossRef]
92. Kryshtafovych, A.; Schwede, T.; Topf, M.; Fidelis, K.; Moult, J. Critical Assessment of Methods of Protein Structure Prediction (CASP)—Round XIV. *Proteins Struct. Funct. Bioinform.* **2021**, *89*, 1607–1617. [CrossRef] [PubMed]
93. Husain, Q.; Fahad Ullah, M. Oxidoreductases: Overview and Practical Applications. In *Biocatalysis: Enzymatic Basics and Applications*; Springer International Publishing: Cham, Switzerland, 2019; pp. 39–55. ISBN 9783030250232.